Proton Transport by Bacteriorhodopsin in Planar Membranes Assembled from Air-Water Interface Films

JUAN I. KORENBROT and SAN-BAO HWANG

From the Departments of Physiology and Biochemistry, University of California School of Medicine, San Francisco, California 94143. S.-B. Hwang's present address is Merck & Co., Division of Membrane and Arthritis, Rahway, New Jersey 07065.

ABSTRACT   Bacteriorhodopsin, in known amounts and controlled orientation, is incorporated into planar membrane films. These films are formed by the sequential transfer of two air-water interface films onto a thin, hydrophilic, electrically conductive support cast from nitrocellulose. The films are easily accessible to electrical measurements and to control of the ionic milieu on either side of the membrane. The area of the assembled membrane films can be varied between 2.3×10^{-2} cm^2 and 0.7 cm^2. Illumination of these films produces photocurrents, photovoltages, and changes in the pH of the surrounding medium. The peak amplitude of the photocurrent increases linearly with light intensity for dim lights, and it approaches a saturating value for brighter lights. In the linear range, the stoichiometry of transport is 0.65 ± 0.06 protons/ absorbed photon. The rate of transport is linearly proportional to light at all intensities tested. The amplitude and kinetics of the photovoltage measured are accurately predicted by the photocurrent generated and the passive electrical features of the film. Parallel measurements of pH and photocurrent reveal that the light-induced changes in pH are fully accounted for by the rate and amount of charge transport across the membrane. Preceding the transport of protons, a transient photovoltage is detected that exhibits no detectable latency, reaches peak in about 80 μs, and probably arises from light-induced intramolecular charge displacements.

INTRODUCTION

Illumination of Halobacteria grown under low oxygen tension results in a simultaneous acidification of the suspending medium and a change in the cell's membrane potential (Bakker et al., 1976; Bogomolni, 1977). Extensive investigations have demonstrated that these effects arise because a structurally specialized region of the plasma membrane of these cells, the purple membrane, contains a protein, bacteriorhodopsin, which functions as a light-activated proton pump (see reviews by Oesterhelt [1975] and Stoeckenius et al. [1979]). Bacteriorhodopsin molecules are the only protein constituents of the purple membrane, and in it they are oriented in a two-dimensional

crystalline lattice (Henderson, 1977). Each protein molecule contains a single covalently bound chromophore, retinal, which renders it sensitive to visible light. Upon absorption of light, the bacteriorhodopsin molecules proceed through a cyclic sequence of at least five different photochemical intermediates. In conjunction with these photochemical changes, the protein molecule transports protons from the intracellular space to the external medium (Stoeckenius et al., 1979).

Important parameters of the function of bacteriorhodopsin remain to be explained. For example, the molecular mechanism of the proton transport is unknown. In addition, there is uncertainty with regard to some physiological parameters of the transport, such as its quantum yield, the relation between proton translocation and changes in the pH of the medium, and the temporal relation between proton transport and the spectrophotometric intermediates in the photopigment (Stoeckenius et al., 1979). Finally, because bacteriorhodopsin in the intact cell operates under changing gradients of ion concentration and electrical potential, it is of interest to determine whether such gradients play a regulatory role in the function of the protein. These questions can be best addressed in simplified model systems consisting of oriented bacteriorhodopsin molecules incorporated into planar films (see review by Korenbrot [1977] and Schreckenbach [1978]).

Planar lipid films containing purple membrane were first formed by Drachev et al. (1974) who "painted" thick films by applying a suspension of membrane fragments and lipid in decane onto a hydrophobic aperture. Drachev et al. (1976) found that these films could be more efficiently formed by adsorbing or "fusing" onto a preformed thick lipid film either isolated purple membrane fragments or liposomes into which purple membrane fragments were first incorporated (proteoliposomes). Shieh and Packer (1976) further improved the system by reinforcing the preformed lipid film with a polymer, thus prolonging its lifetime. Much greater stability has been obtained by adsorbing purple membrane fragments onto thick lipid films formed by impregnation of solid supports such as Millipore filter membranes (Blok et al., 1977; Blok and Van Dam, 1978) or collodion membranes (Drachev et al., 1978). Dancshazy and Karvaly (1976) first described the adsorption of purple membrane fragments onto thin lipid films. All these model systems have been extremely useful and have provided important information on the function of bacteriorhodopsin. However, they have important limitations in their analytical use. A critical limitation was first pointed out by Drachev et al (1976): the adsorption onto a preformed lipid film results in a physical system best described as two membranes, one a purple membrane the other a lipid film, arranged in series. The two membranes form a sandwichlike structure in which each maintains its characteristic impedance. Thus, the purple membrane is directly accessible to the aqueous phase on only one of its surfaces. The elegant work of Hermann and Rayfield (1978) and Bamberg et al. (1979), who measured the photocurrents generated by adsorption of either proteoliposomes or isolated purple membrane fragments onto preformed lipid bilayers, has quantitatively demonstrated that such is the case. In addition, none of the

available model systems allow control of the number or orientation of the bacteriorhodopsin molecules in the model membranes. Because of these limitations we undertook the development of an alternative experimental method that would permit the formation of planar films of large and variable area, and containing known amounts of oriented, crystalline bacteriorhodopsin. Furthermore, the films were to be easily accessible to electrical and spectrophotometric measurements, and to the complete control of the ionic milieu on either side of the membrane. We describe here this new experimental method, which consists of the sequential transfer of two air-water interface films onto a hydrophilic, electrically conductive support. This method, we find, will be applicable to other membrane proteins as well. We further describe our measurements of quantum efficiency of proton transport and the relation between pH change and proton transport, and we report the detection of transient, light-induced charge displacements in bacteriorhodopsin.

MATERIALS AND METHODS

Materials

Purple membrane fragments were isolated from *Halobacterium halobium* R_1 and purified according to Oesterhelt and Stoeckenius (1974). The purified fragments were stored at 4°C in basal salt solution (4.3 M NaCl, 0.275 M KCl, 0.080 M MgSO$_4$, 0.009 M sodium citrate, pH 7.0). Phosphatidylcholine (PC) from soya beans was obtained from Netterman Gmbh (W. Germany), repurified, and stored as described previously (Hwang et al., 1977 *a*). Isoamyl acetate (99% pure) was obtained from Aldrich Chemical Co. (Milwaukee, Wis.) and used as received. Hexadecane (99% pure) was purchased from Sigma Chemical Co. (St. Louis, Mo.). Nitrocellulose (strips of purified Parlodion) were obtained from Mallinckrodt Inc. (Los Angeles, Calif.). Polyester film (127 μm thick) was purchased from Transilwrap Corp. (San Francisco, Calif.). Water used throughout was once glass distilled and then purified with the use of a sequence of ion-exchange resin beds, activated charcoal, and Millipore filters (Milli Q distillation apparatus, Millipore Corp.).

Methods

SURFACE BALANCE   A Langmuir surface balance consisting of a rectangular, shallow Teflon (E. I. Du Pont, de Nemour & Co., Wilmington, Del.) trough (outside dimensions, 40 × 12.5 × 2 cm; inside dimensions, 36.5 × 10.5 × 0.8) and a tight-fitting surface barrier was constructed (Fig. 1). At one end of the trough a cylindrical well (radius 2.25 cm, depth 3 cm) was made. To permit illumination, a glass-sealed porthole (radius 0.75 cm) was machined on the wall of the well. Surface pressure was measured by the Wilhelmy method (Gaines, 1966) using platinum foil as the detector plate. A digital servomechanism coupled the surface pressure detection system to the motor controlling the motion of the surface barrier. This mechanism permitted the quick (time constant of response <100 ms) and automatic motion of the surface barrier as needed to maintain a given surface pressure within ±0.05 mN/m. The surface balance was enclosed within an electrically shielded box and was supported on a mechanical stage designed for vibration isolation.

GLASS CHAMBERS AND THEIR PREPARATIONS FOR MEMBRANE ASSEMBLY   The glass chambers used were custom built of Pyrex glass and are shown in Fig. 2. They

consisted of an open cylinder (1.5 cm i.d. × 1.7 cm o.d., 2.5 cm long) with flared ends (o.d. of the flare, 2.5 cm). Three glass tubes (3 mm i.d. × 5 mm o.d.) were fused to the cylinder, a central one (7 cm long) and two lateral ones (2 cm long), each forming an angle of approximately 45° with the central one. To ready them for the assembly of membranes, the chambers were cleaned by immersion in a boiling solution of detergent, rinsed extensively, and then immersed in a warm solution of chromate in sulfuric acid (Chromerge, Monostat Corp., New York). The chambers were then exhaustively rinsed under running distilled water and dried in an oven. A disk of polyester film (diameter, 13 mm; 127 μm thick) was glued onto one end of the glass chamber with a quick-setting epoxy mixture (5 Minute epoxy from Devcon Corp., Danvers, Mass.). This polyester disk had a hole in its center. Two hole sizes were used: $2.3 \pm 0.1 \times 10^{-2}$ cm^2, made by slowly applying to the polyester film an electrically heated, smooth platinum tip, (diameter at the tip, 0.3 mm) or 0.7 cm^2, made with a metal punch. The polyester disks were cleaned with detergent and rinsed extensively with water before their attachment to the glass chamber. The epoxy glue was allowed to dry for 2–4 h. A thin nitrocellulose film was then deposited across the
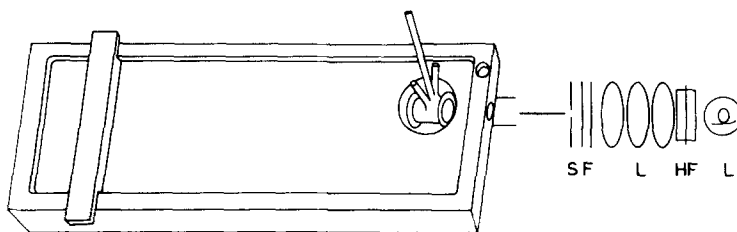

FIGURE 1.   Schematic drawing of the Langmuir surface balance. At one end of the Teflon trough, a well was made to acommodate the glass chamber. Stimulus light was delivered through a glass porthole in the well. The photostimulator consisted of a lamp, (L), a water-jacketed heat filter (HF), a series of lenses (L) that focused the light beam on the entrance slit of a fiber bundle, an electronic shutter (S) and a holder to accommodate neutral-density and interference filters (F).

hole in the polyester disk (details below). After a drying time of 1–3 h, a glass disk was glued in place to seal the remaining open end of the glass chamber. The glass disks (2.5 cm in diameter, 0.18–0.22 mm thick, Thomas Scientific Co., Philadelphia, Pa.) were cleaned with the procedure used for the glass chambers and glued with the quick-setting epoxy.

pH GLASS CHAMBER   The pH glass chamber was custom built by Ingold Electrodes Co. (Lexington, Mass.) and is illustrated in Fig. 2. It consisted of a closed, cylindrical glass chamber (1.7 cm in diameter, 1.2 cm long) with a single stem (0.8 cm in diameter and 6 cm high) containing a reference electrolyte. One end of the chamber was constructed of pH-responsive glass. To ready the chamber for the assembly of membranes, it was first cleaned with detergent followed by rinsing with ethanol and running distilled water. The chamber was allowed to air dry (30 min), and a thin nitrocellulose film was then deposited across the pH-responsive glass surface.

CASTING AND DEPOSITION OF NITROCELLULOSE FILM   Nitrocellulose is a nitrated derivative of cellulose that contains 10.5–12% nitrogen (approximately two nitrates per glucose). A 1% (wt/vol) solution of purified nitrocellulose in isoamyl acetate was

prepared by overnight stirring at room temperature in a closed glass container. This solution was used within 1 week of its preparation and then discarded. Thin films were prepared by either of the two following procedures, depending on the electrical features desired in the film. One procedure was based on the method described by Carnell and Cassidy (1961): A glass disk (2.5 cm in diameter, 0.18–0.22 mm thick) was cleaned as described above for the glass chambers. The solution of nitrocellulose (50 ml) was placed in a clean glass vessel and the glass slide, held perfectly vertical, was mechanically dipped into the solution at a rate of 0.16 cm/s. The slide was held under the solution for 2 min and then withdrawn at a rate of 0.077 cm/s. The polymer
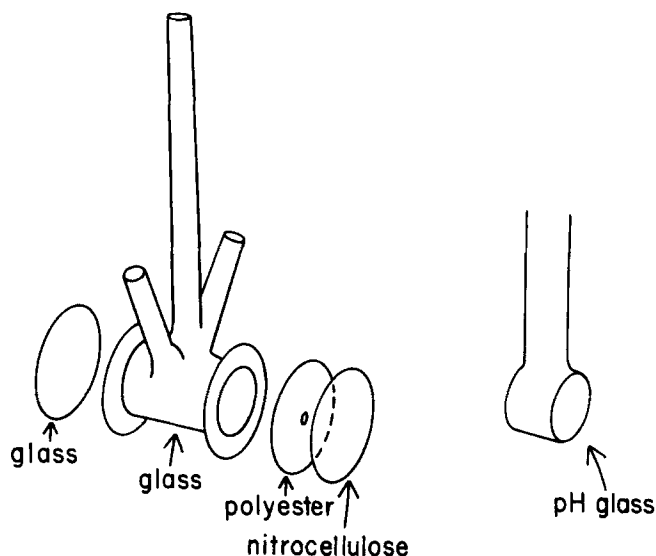

FIGURE 2. Schematic drawing of the glass chamber and pH electrode chamber used for the membrane assembly. The glass chamber consisted of an open cylindrical body the ends of which were closed on one side by a glass disk and on the other by a polyester disk. The polyester disk served as support for the thin nitrocellulose film onto which the model membranes were assembled. The open vertical arms of the glass chamber accommodated electrodes and allowed the exchange of the solution contained in the chamber. The pH electrode chamber was constructed with pH-sensitive glass on its front face. This chamber contained an Ag–AgCl electrode and an indifferent electrolyte and was permanently closed.

film was allowed to dry away from the vapors of the polymer solution for precisely 90 s. At the end of that time, the nitrocellulose film was floated off the glass by manually dipping the slide, held at about 45°, into a glass vessel filled to the brim with water. The floating nitrocellulose film was transferred onto the glass chambers, across the face of the polyester support, by manually inserting the chamber in the aqueous bulk and then withdrawing it under the film at a 60° angle. 1–2 h later, any uncovered polyester surface was covered with a thin coat of polymer solution applied with a disposable glass capillary. The second film-casting procedure was based on the method of Lackshminarayanaiah and Shanes (1965): The glass chambers were first immersed in 400 ml of a 0.1 N NaCl aqueous solution contained in a glass vessel. The surface

area of the solution was 76 cm². The glass vessel was covered, and through an aperture in the cover, sufficient 1% polymer solution was applied onto the aqueous surface to produce a 360-Å-thick film (density of nitrocellulose is 1.66 g/ml (Weast, 1971). 30 min were allowed for solvent disappearance and formation of the polymeric film. At the end of that time, the glass chamber was withdrawn across the aqueous surface at a 60° angle. Polymer film covering nonpolyester surfaces was easily wiped off. Again, any uncovered polyester surface was covered 1-2 h later. Both procedures were carried out in an air-conditioned room at ambient temperature (19-21°C) and humidity and in the absence of any air currents.

TABLE I

PHYSICAL CHARACTERISTICS OF NITROCELLULOSE
SUPPORT FILM

Dry thickness		$360\pm10\text{Å}$*	
Index of refraction at 630 μm		1.455	
Electrical resistance			
Carnell and Cassidy		$7\pm5\times10^3$ Ω cm²‡; $2\pm3\times10^3$ Ω cm²§	
Lackshminarayanaiah and Shanes		$9\pm6\times10^3$ Ω cm²‡; $8\pm5\times10^2$ Ω cm²§	
Capacitance		0.156 μF/cm²‖	
Transfer numbers			
			In aqueous solution¶
NaCl	t_{Na}	0.409 ± 0.028**	0.391
	t_{Cl}	0.590 ± 0.029	0.609
KCl	t_K	0.498 ± 0.002	0.490
	t_{Cl}	0.501 ± 0.002	0.510
HCl	t_H	0.817 ± 0.013	
	t_{Cl}	0.182 ± 0.13	

* The average and range of measurements made on four different films, each film being sampled with a laser beam at three random positions.

‡ Measurement made in 4 × 10^{-4} M NaHCO₃, 4 × 10^{-4} M CdCl₂.

§ Measurement made in 4 × 10^{-4} M NaHCO₃, 4 × 10^{-4} M CdCl₂, 50 mM NaCl.

‖ Calculated from the thickness and dielectric constant of the film (ϵ = 6.7 [Weast, 1971]), a procedure fully validated by Lackshminarayanaiah and Shanes (1965).

¶ Data taken from Robinson and Stokes (1959).

** The transfer number given is the average of four measurements carried out in bionic cells (10:100 mM or 50:500 mM) of the salt indicated. These numbers were measured in a Carnell-Cassidy film only.

PHYSICAL PROPERTIES OF NITROCELLULOSE FILMS   The thickness and uniformity of dry films were measured in collaboration with Dr. J. Swalene of the IBM Research Center (San Jose, Calif.) by the technique of surface plasmon spectroscopy (Pockrand et al., 1977). The DC electrical resistance was determined by measuring transfilm current in response to applied steps of voltage. Ion selectivity and ion transfer numbers were established by measuring both dilution potentials and biionic potentials. Some salient physical features of the films are listed in Table I. The films are thin and extremely uniform. As indicated by their low electrical resistance, the films are highly permeable to ions and their current-voltage characteristics are linear up to ±1 V. The films do not exhibit selectivity among the various cations and anions tested, and ion transfer numbers are nearly the same as those measured in aqueous solution. The electrical resistance of nitrocellulose films deposited on the polyester support across

apertures of various radii is inversely proportional to the area of the aperture. This demonstrates that the flow of current across nitrocellulose supported by polyester occurs only across the open hole and thus that tangential currents in the nitrocellulose are negligible.

ELECTRICAL MEASUREMENTS OF TRANSPORT   Electrodes used in these experiments consisted of Ag/AgCl sintered pellets (In-Vivo Metrics, Healdsburg, Calif.) connected to the solutions via 2 M KCl–agar bridges. The Ag/AgCl pellets were shielded from light. Membrane voltage was measured with a high-input impedance differential amplifier (model 1090, Winston Electronics, San Francisco, Calif.) Short-circuit membrane current was measured with an FET operational amplifier module (model 380K, Intec Corp., San Jose, Calif.) assembled in a current-to-voltage conversion mode. Membrane resistance was measured with a bridge circuit coupled to the membrane voltage detection probe, which permitted measurement of membrane voltage in response to variable steps of current (model BR-1, Winston Electronics, San Francisco, Calif.). The pH electrode signal was recorded with the same high-input impedance amplifier used for recording membrane voltage. The signals of the various amplifiers described above were further amplified, digitized, and averaged in a signal averaging computer (model 1070, Nicolet Instrument Corp. Madison, Wis.) and stored on digital tape.

PHOTOSTIMULATOR   Two different light sources were used in these experiments. One was a Xenon arc flash source (U. S. Scientific Instruments, Inc. Boston, Mass.) of $\sim$10 μs duration, and the other was a DC-powered, 300 W tungsten-halogen lamp. An optical bench collimated and focused the light at the entrance of a fiber bundle (1.25 cm in diameter, 30 cm long), the exit of which was next to the glass porthole in the well of the surface balance (see Fig. 1). The duration and repeat frequency of the light stimuli were controlled with an electromagnetic shutter. Their intensity and spectral composition were controlled with neutral-density (Melles-Griot, Irvine, Calif.) and narrow-band interference filters (Baird-Atomic Inc., Bedford, Mass.). Except where otherwise noted, photostimuli consisted of visible light at wavelengths >480 nm. Light intensity was measured with a calibrated photodiode (United Detector Technology, Inc., Santa Monica, Calif).

PRODECURE OF MEMBRANE ASSEMBLY
1) Formation of Purple Membrane-Lipid Interface Film
Films of purple membrane and lipid were formed at a clean air-water interface according to previously detailed procedures (Hwang et al., 1977 *a*). Briefly, the interface films were formed by applying onto a clean water surface a suspension of purple membrane fragments in a solution of soya PC in hexane. The amount of purple membrane in the organic phase suspension, and thus in the interface film, can be experimentally controlled by varying, for a constant amount of soya PC, the weight ratio of bacteriorhodopsin to lipid. In the experiments reported here two specific weight ratios were tested 7:1 and 3.5:1 (bacteriorhodopsin:soya PC). A fresh membrane suspension was prepared for each membrane assembled.
2) Assembly
Completely assembled glass chambers were used not sooner than 12 h nor later than 3 d after being completed. Immediately before use, the chambers were cleaned by gently dripping redistilled hexane over them. Hexane was allowed to evaporate (10 min), and the chambers, with their inside dry, were then immersed in the surface balance. All assembly procedures were carried out with films formed over an aqueous subphase consisting of 4×10^{-4} M $CdCl_2$, 4×10^{-4} M $NaHCO_3$, pH 5.8. The chamber

was held vertically in the cylindrical well. The purple membrane–lipid interface film was then spread and brought to a surface pressure of 30 mN/m. While that pressure was held with the aid of the servomechanism, the glass chamber was mechanically withdrawn at the rate of 0.015 cm/min. The surface film transfer onto the glass chamber was monitored by the automatic motion of the surface barrier. After the glass chamber was withdrawn, the aqueous surface was cleaned. A second lipid film was spread (40 µl of a hexane solution of soya PC, 0.5 mg/ml, and hexadecane, 4.5 mg/ml). These operations took 4–6 min. The lipid film was then collapsed to a surface pressure of 30 mN/m. After 10–12 min, the glass chamber was moved downward through the lipid interface film at a rate of 0.015 cm/s. The glass chamber was stopped when the hole in the polyester film was aligned with the glass porthole used for illumination. At that time aqueous solution was added to the inside of the glass chamber and the electrodes were placed in their appropriate positions.

RESULTS

The strategy in the method of membrane assembly we describe here is to sequentially transfer two air-water interface films onto a hydrophilic, electrically conductive support. Table I describes some physical features of the polymeric matrix we utilized to support the assembled membrane films.

The first interface film transferred onto the hydrophilic support consisted of oriented, nonoverlapping single-sheet fragments of purple membrane separated by a lipid monolayer. The membrane fragments are typically 0.1 µm in diameter and, at 7:1 bacteriorhodopsin to soya PC weight ratio, they randomly occupy ~35% of the aqueous surface. We have previously described in detail the structural, spectroscopic, and functional characteristics of these films and have established that bacteriorhodopsin molecules are fully functional within them (Hwang et al., 1977 a and 1977 b). We followed the effective transfer of the interface film from the water surface onto the solid support by measuring, at constant surface pressure, the surface area loss during transfer. The transfer of all films was carried out at 30 mN/m, a pressure at which the films were stable. The purple membrane interface films transferred onto the support glass chamber with a transfer ratio (surface area loss:area of solid support) essentially of 1 ($n = 25$).[1]

For the second interface film in the membrane assembly, we initially attempted the transfer of a soya PC monolayer. The transfer, however, was erratic. Following the suggestion of White et al. (1976), we gave attention to satisying the contact angle requirements necessary to assemble lipid bilayers from monolayers. White et al. (1976) suggested that these requirements might be satisfied by retaining a small amount of hydrocarbon solvent in the interface film while transfer takes place. Since hexadecane evaporates from mixed lipid-solvent interface films at a rate that can be determined (Gaines, 1961) (see Appendix I), we followed the suggestion of White et al. by forming the second interface film from a hexadecane–soya PC mixture and allowing sufficient time for most, but not all, the solvent to disappear before beginning

[1] Because of the odd shape of the glass chamber we could not accurately determine the film transfer ratio and this number can be considered reliable only to within ±10%. Transfer ratio onto glass slides was 1.

the transfer. The mole ratio of the hexadecane:soya PC mixture used was 32:1, and we started the transfer 10–12 min after spreading the film (see Appendix I). The presence of the remaining hydrocarbon permitted the successful transfer of the second (lipid) interface film. The transfer ratio of the second film was 0.59 ± 0.09 ($n = 25$). It must be remembered that in the first interface film ~35% of the surface consists of purple membrane fragments and must, therefore, be hydrophilic and cannot be expected to interact with the hydrophobic surface of the second film. After the membrane assembly was completed, we waited another 10 min before we began recording electrical data. This was sufficient time to allow all the hexadecane remaining on the surface to disappear. Although some hydrocarbon may remain in the assembled membrane, it must have been a very small quantity inasmuch as most of it had disappeared from the interface and since it is excluded from lipid bilayers (White, 1978). This procedure of membrane assembly, thus, produced planar films containing known amounts of oriented single-sheet fragments of purple membrane incorporated in a lipid bilayer and separating two easily accessible aqueous compartments.

Photocurrent and Photovoltage

Typical transmembrane currents and voltages produced by step illumination of various intensities of a membrane (2.3×10^{-2} cm^2) assembled from a 7:1 bacteriorhodopsin:soya PC weight ratio interface film in a low-salt solution (4×10^{-4} M CdCl$_2$, 4×10^{-4} M NaHCO$_3$, pH 5.8) are shown in Fig. 3. The sign of both signals indicates the transfer of positive charge in the light from the outside to the inside of the glass chamber. The photocurrent (and the photovoltage) exhibits the same general features. At high light intensities, the responses generally appear as a transient that reaches a peak proportional to light intensity and then decays to a small steady state with a time constant proportional to light intensity. At low light intensities, the transient is much less pronounced. The photoresponses also exhibit a transient at the termination of the light pulse.

The electrical photocurrents observed in the assembled membranes are produced by photoexcitation of the light-adapted form of bacteriorhodopsin, since their action spectrum, illustrated in Fig. 4, matches the absorption spectrum of the photopigment.

The wave form of the short-circuit photocurrent recorded in the low-salt solution arises from the fact that the assembled membrane is supported by a polymeric film that exhibits a characteristic electrical capacitance and resistance. Thus, the appropriate electrical equivalent circuit of this model system, shown in Fig. 5, consists of the assembled membrane of resistance R_1 and capacitance C_1 and which contains the current generator I_{BRh} in series with a film of resistance R_2 and C_2. The values of R_2 and C_2 are experimentally determined and listed in Table I. R_1 was measured directly and found to be $2 \pm 1 \times 10^5$ Ω cm^2 ($n = 21$). An analysis of the circuit appears in some detail in Appendix II. Upon illumination, positive charges are pumped into the space between the assembled membrane and the nitrocellulose support. This

pump current has a steady value, I_{BRh}, throughout the light pulse. The accumulation of pumped charges results in the generation of a potential across the polymeric film. The observed short-circuit current, I_0, consists of a leakage current through R_2 and a capacitative current through C_2 driven by the generated potential. As this generated potential approaches a steady-state value, the capacitative current decays leaving only the steady-state current.
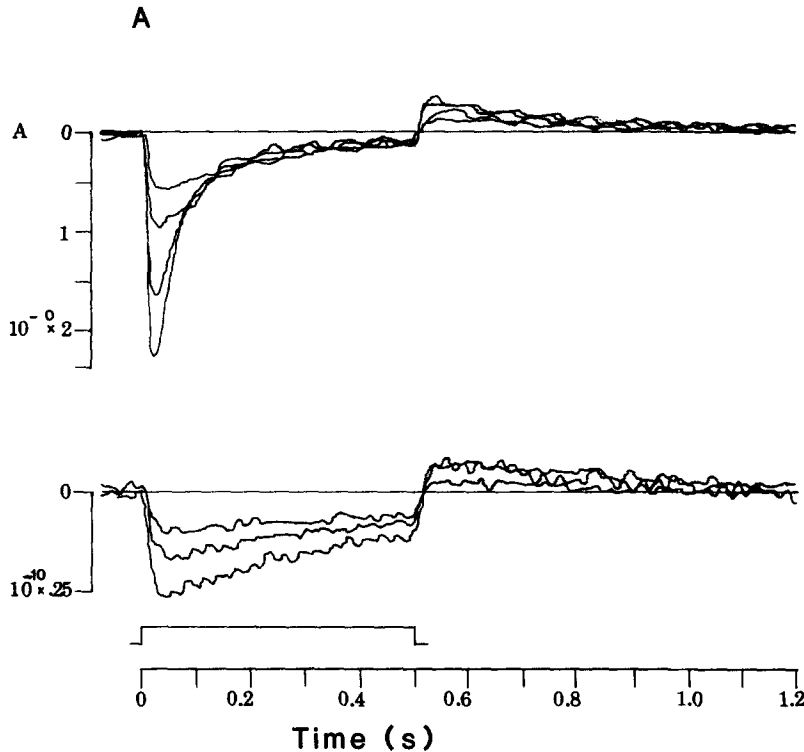
A

FIGURE 3. Photocurrents (A) and photovoltages (B) measured in a 2.3×10^{-2} cm^2 membrane in 5×10^{-4} M NaHCO$_3$, 5×10^{-4} M CdCl$_2$, pH 5.8. The stimulus light was filtered through a 3-71 filter (Corning Glass Works) that passed all wavelengths above 480 nm. The curves shown were recorded in response to step illumination of the following intensities in decreasing order: 49, 30.9, 15.5, 7.75, 2.45, 1.55, and 0.77 mW/cm^2. The responses to low light intensities are plotted with four times the vertical gain of those to high light intensities.

When the light is turned off, the current pump stops, and the generated potential returns to zero. As a consequence, the capacitative current is again observed but in the opposite polarity. If the capacitative current at off is larger than the leakage current, the net observed current reverses sign and then decays to the baseline.

In Appendix II it is shown that the observed short-circuit photocurrent, I_0,

is proportional to the pump current I_{BRh} and given by (see Appendix II for definition of constant)

$$I_o = I_{BRh} \frac{C_2}{C} \left(A + (1 - A) e^{-t/\tau} \right). \tag{1}$$

Eq. 1 indicates that, as observed, the photocurrent should reach a peak amplitude and then decay with a time constant, τ, to a steady-state value.
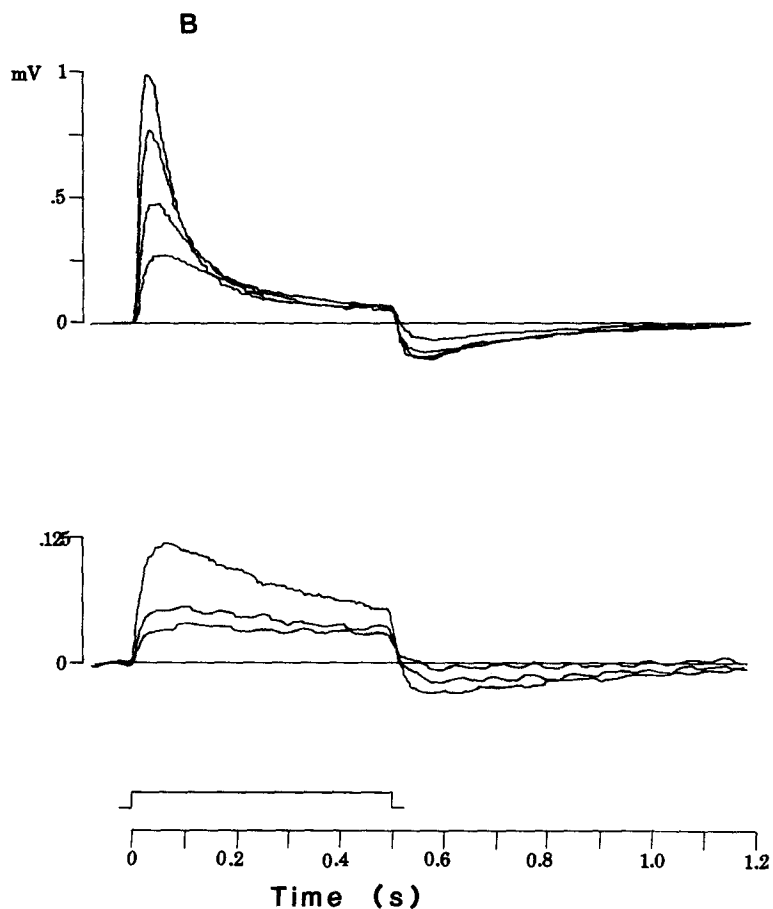
B

FIGURE 3.

The value of the observed steady-state photocurrent, $I_o^{steady\ state}$, is proportional to the pump current, the assembled membrane resistance, and the nitrocellulose film resistance. From Eq. 1 and the appendix:

$$I_o^{steady\ state} \alpha\ I_{BRh} \cdot \frac{R}{R_2}. \tag{2}$$

At low salt concentrations, the relatively high resistance of the polymeric

support permits only a small photocurrent to be observed in the steady state. However, one of the purported advantages of the present assembly method is that the polymeric support should allow easy control of the ionic solutions bathing the membrane. As a consequence, the resistance of the polymeric support should also be under experimental control by simply varying the salt concentration in the aqueous solution. This is indeed the case. In Fig. 6 are shown photocurrents measured in the presence of various salt concentrations.
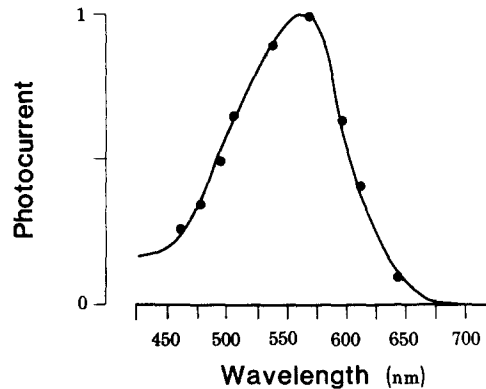
FIGURE 4.   Action spectrum of the photocurrents measured in a 2.3×10^{-2} cm^2 assembled membrane. To obtain each point, we recorded photocurrents in response to step illumination of various intensities at each wavelength tested. From that data, the peak photocurrent in response to a constant number of photons at each wavelength was determined. The data shown were normalized by defining the current measured at 570 nm as unity.
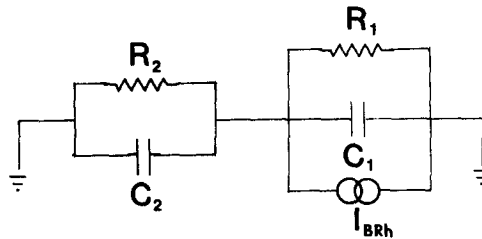

FIGURE 5.   Equivalent circuit diagram of the assembled membranes when short-circuit currents are measured. R_1 and C_1 represent the resistance and capacitance of the model membrane containing the purple membrane fragments in which the current generator I_{BRh} is located. R_2 and C_2 are the resistance and capacitance of the nitrocellulose film.

All data were recorded across the same membrane assembled from 7:1 bacteriorhodopsin:lipid films across a 2.3×10^{-2}-cm^2 aperture. This membrane was assembled on a nitrocellulose film cast by the Lackshminarayanaiah-Shanes (1965) technique. In this experiment, the membrane was assembled in the usual manner, and the salt concentration was changed by simply exchanging the solutions inside, but not outside, the glass chamber (thus creating a gradient in salt concentration). The data in Fig. 6 demonstrate that, as
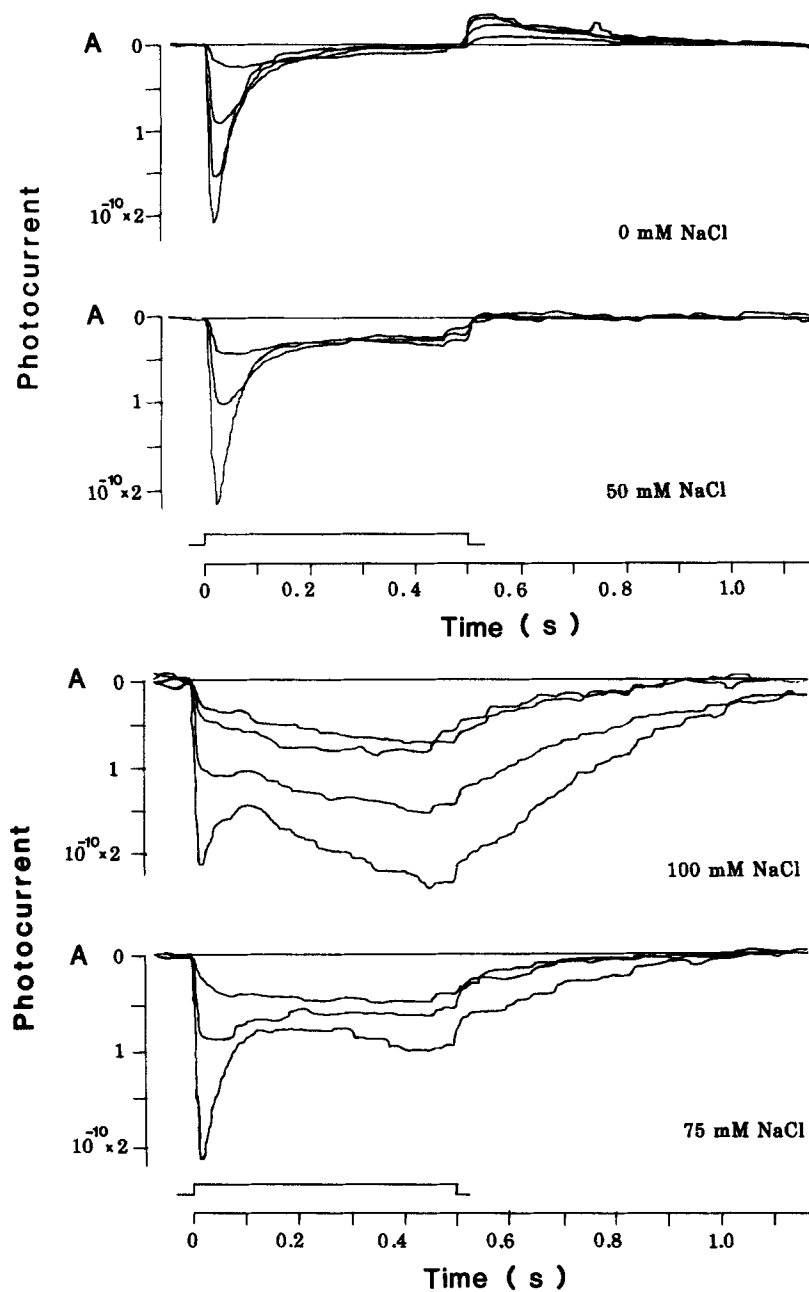
FIGURE 6. Effect of aqueous salt concentration on photocurrents recorded across a 2.3×10^{-2} cm^2 membrane assembled from 7:1 bacteriorhodopsin:lipid films. NaCl was added to 4×10^{-4} M NaHCO$_3$, 4×10^{-4} M CdCl$_2$, pH 5.8, in the concentrations indicated, and the solution on the inside of the glass chamber was exchanged. The solutions were exchanged in random order. The photocurrents were recorded immediately after the solution exchange. The records shown were obtained in response to illumination of 49, 30.9, 15.5, and 7.75 mW/cm^2.

expected, increasing the salt concentration, which decreases the nitrocellulose resistance, R_2 (Lackshminarayanaiah and Shanes [1965] and Table I), increases the steady-state component of the current without effectively modifying the capacitative component. Thus, bacteriorhodopsin membranes assembled on polymeric support are accessible to the aqueous environment on both sides.

It follows from the equivalent electrical circuit (Fig. 5) that the wave form of the photovoltage recorded across assembled membrane should be accurately predicted by simply convoluting the recorded photocurrent with a one-stage resistance-capacitance (RC) filter, where the value of R and C are defined in Appendix II. The amplitude of the photovoltage should be given by the
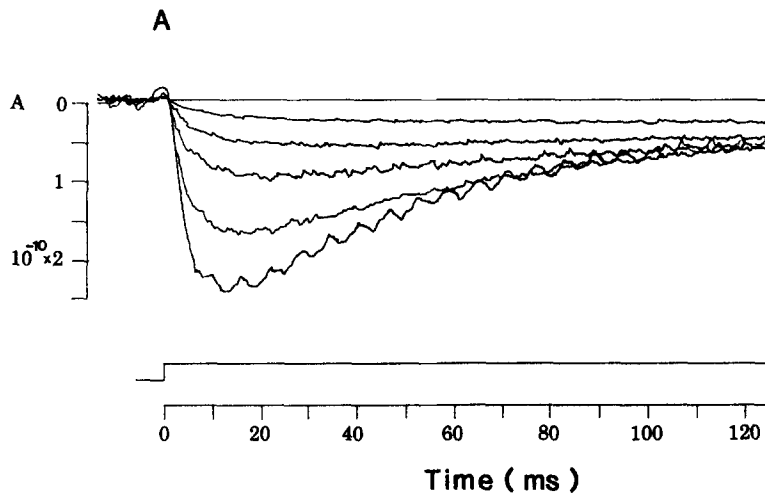
A

Time (ms)

FIGURE 7. Photocurrents (A) and photovoltages (B) recorded across a 2.3 × 10^{-2} cm^2 membrane assembled from 7:1 bacteriorhodopsin:lipid films. Shown are responses to stimuli of 49, 30.9, 15.5, 7.75, and 2.45 mW/cm^2. Superimposed in B are recorded photovoltages and smooth curves obtained by convoluting the experimentally recorded photocurrents through a one-stage RC filter of appropriate time constant. The time constant used was 24 ms. For clarity, C displays the computed photovoltages alone.

amplitude of the photocurrent and the value of R. Thus,

$$V = R \cdot \frac{1}{\tau} \cdot \int I(t') \, e^{-(t - t')/\tau} \, dt'. \tag{3}$$

Fig. 7 illustrates a set of photocurrents and photovoltages recorded across the same membrane. Also illustrated are records generated using digital computation in which the photocurrents have been integrated through a one-stage RC filter with a time constant selected to best match the observed photovoltages. The fit of the simulated and recorded photovoltages is excellent, and was so for all data tested (11 membranes). The value of the resistance of the

assembled membrane estimated indirectly from the amplitude of the photo-voltage and the time constant selected for best fit was in close agreement with the value obtained through direct measurement (see above). The amplitude and wave form of the photovoltage, thus, are defined by the photocurrent and the electrical features of the assembled membrane.

Functional Characterization of the Assembled Films

The experiments described in the following sections were all carried out on Carnell-Cassidy supports and in low-salt solutions to avoid confusion resulting from salt gradients. The specific effects of salt gradients will be investigated in a future report.
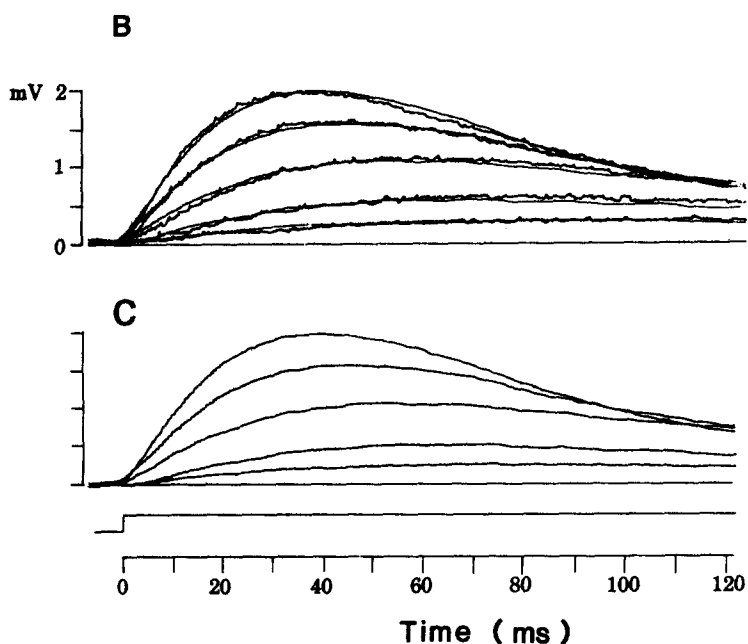

FIGURE 7.

The peak amplitude of the photocurrent (and of the photovoltage) is proportional to light intensity (Fig. 8). At low light levels, both current and voltage are linearly proportional to light intensity (J). At higher levels of illumination the peak current (and voltage) amplitude approaches a saturating value and its dependence on light is best described by a rectangular hyperbola or Michaelis-type relationship, as revealed by the linear dependence of $1/I_m$ (or $1/V_m$) on $1/J$. Thus,

$$I_m = K_1 \cdot J \quad \text{for} \quad J < 3.5 \text{ mW/cm}^2, \quad \text{and} \tag{4}$$

$$I_m = \frac{I_m^{\text{sat}} J}{J + K_2} \quad \text{for} \quad J > 3.5 \text{ mW/cm}^2. \tag{5}$$

Fig. 9 illustrates the dependency on light intensity of the initial rate of rise of the photocurrent, measured as the tangent to the rising phase of the photoresponse. This initial rate of rise has the same form as the initial response of the current generator and is, therefore, a measure of the rate of proton
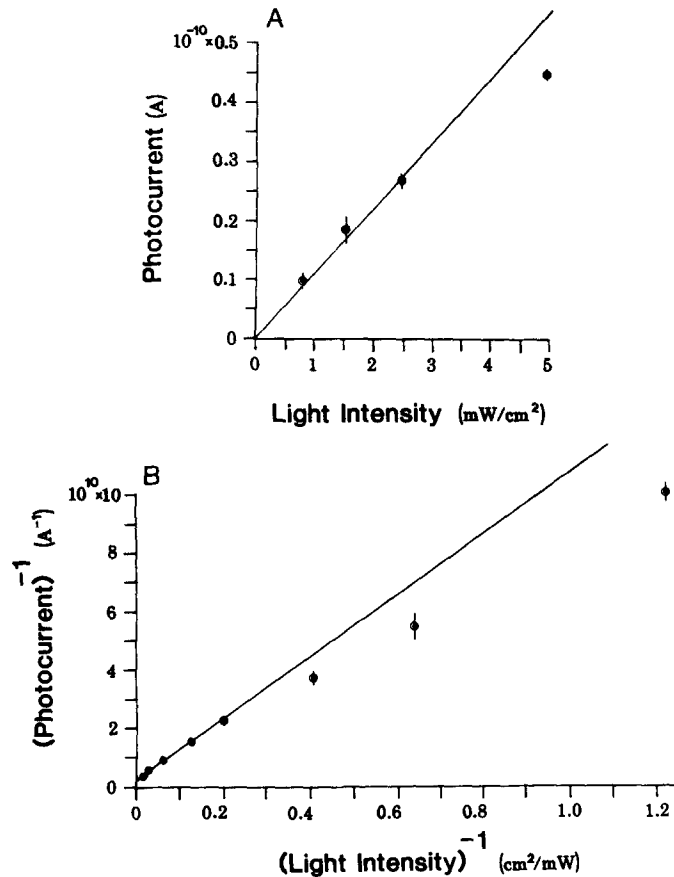

FIGURE 8.   Dependence of peak photocurrent amplitude on light intensity in 2.3×10^{-2} cm^2 membranes assembled from 7:1 bacteriorhodopsin:lipid interface films. A is a linear plot. B is a linear plot of the reciprocal of the current and the reciprocal of the light intensity. The data points surrounded by circles are plotted on both graphs. The amplitude of the current increases linearly with light intensity at low light levels and then approaches a saturating value with a hyperbolic dependence on intensity. Data points are the average of four membranes; error bars indicate ±SD.

translocation. We find that the rate of transport is proportional to light intensity at all light levels tested. This observation indicates that as light intensity increases over the range tested here the number of pumping units (bacteriorhodopsin molecules) activated increases proportionally, with no apparent cooperativity.

Effects of Membrane Area and Protein Concentration

We further tested the quality of the membrane assembly procedure by examining the effects of changes in membrane area and protein concentration on the membrane photoresponse. If the assembly model is adequate, it would be expected that the amplitude of the photocurrents, but not photovoltages,
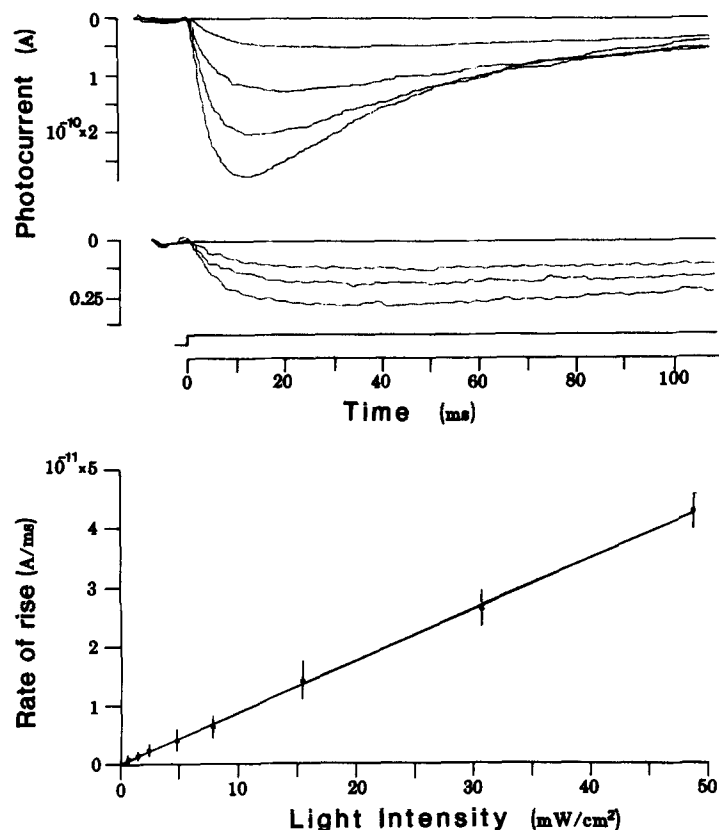

FIGURE 9. Dependence of the rate of rise of the photocurrents on light intensity in 2.3×10^{-2} cm^2 membrane assembled from 7:1 bacteriorhodopsin:lipid films. The records shown were obtained in response to stimuli of 49, 30.9, 15.5, 7.75, 2.45, 1.55, and 0.77 mW/cm^2. The responses to low light intensities are plotted with four times the vertical gain of those to high light intensities. The graph is a linear plot. The data points are the average of four membranes; error bars indicate ± SD.

should scale linearly with the assembled membrane area for a constant surface density of bacteriorhodopsin molecules. In contrast, at a constant membrane area both current and voltate amplitude should scale linearly with the amount of protein in the membrane. These expectations are indeed met.

Fig. 10 illustrates photocurrents recorded across membranes assembled either from 7:1 bacteriorhodopsin:lipid interface films on a 0.7 cm^2 aperture

or from 3.5:1 bacteriorhodopsin:lipid films on a 2.3 × 10^{-2} cm^2. The wave forms of the photocurrents recorded across the two membranes are very nearly the same (they are also very similar to the data illustrated in Fig. 3); however, the magnitudes of the currents are vastly different. The similarity of the recorded wave forms indicates that, as expected, the molecular features of charge transport by bacteriorhodopsin are independent of membrane area or protein concentration. To compare quantitatively the amplitude of the photocurrents recorded in the various membranes, we measured the peak amplitude and normalized it to a unit area of membrane and a unit of optical absorbance at 570 nm. Membrane area was measured under a microscope and the absorbance at 570 nm was taken from direct spectrophotometric measurements of the purple membrane interface films reported previously (Hwang et al., 1977 a). The absorbance at 570 nm is, of course, a direct measurement of protein concentration. Fig. 10 illustrates the dependence of
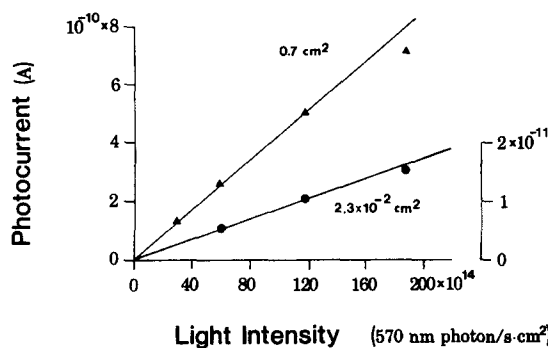

Light Intensity (570 nm photon/s·cm²)

FIGURE 10. Dependence of photocurrent peak amplitude on the number of photons of 570 nm wavelength delivered per unit time per unit area by the stimulus light. Shown are data measured in membranes of either 2.3 × 10^{-2} cm^2 or 0.7 cm^2 area assembled from 7:1 bacteriorhodopsin:lipid films. The calibration on the right applies to the data of the small membranes.

the normalized photocurrent peak amplitude on light intensity as measured in membranes of various areas and protein concentrations. The normalized photocurrents at all intensities tested yield essentially the same value regardless of the membranes from which they were obtained. That is, the amplitude of the photocurrent does scale linearly with bacteriorhodopsin content (at constant area) or membrane area (at constant bacteriorhodopsin surface density). In addition, it is apparent in Fig. 10 that the light-intensity dependence of the photocurrent amplitude is the same in all membranes assembled. That is, the stoichiometry of charge transport, as expected, does not depend on the area of the assembled membrane or on its bacteriorhodopsin content. Similarly, but not shown, the dependence on light intensity of the normalized rate of rise of the response is the same in all membranes assembled (see Fig. 9). In all the membranes, the photovoltages recorded are accurately simulated by convoluting the recorded photocurrents with a one-stage RC filter. It is apparent from the data, then, that the method of assembly described here permits

control of the area and of the amount of protein incorporated into planar membrane films.

Photo-pH Response

The assembled bacteriorhodopsin membranes were studied to determine whether light-induced changes in pH produced by the photopigment can be quantitatively accounted for by transported charges, or whether additional binding and/or release of protons may occur in the light. The sign of the photocurrent indicates that positive charges are transferred toward the nitrocellulose film. Therefore, we assembled membranes directly on a pH-responsive glass surface coated with a Carnell-Cassidy polymeric film (see Fig. 2). The proton concentration changes produced by step illumination of membranes assembled from 7:1 (bacteriorhodopsin:soya PC) film are illustrated in Fig. 11. The pH decreases in the face of the electrode during illumination and returns to its starting value at the termination of the stimulus, thus indicating the net transfer of protons toward the electrode surface. To confirm that the response of the pH electrode indeed reflects a change in proton concentration, we recorded a pH photoresponse under typical conditions and compared it with a second response of the same membrane after increasing the buffering power of the solution bathing it. The *inset* in Fig. 11 illustrates typical results of such experiments. The data shows that, as expected from a true pH response, the photoresponse in the more strongly buffered solution is smaller in amplitude than that in the less well buffered solution, but it does not change in wave form. The magnitude of the reduction of the photoresponse is proportional to the change in buffering power of the solution. The pH photoresponse exhibits an action spectrum that matches the absorption spectrum of the light-adapted form of bacteriorhodopsin (not shown, but similar to data in Fig. 4). Thus, illumination of the assembled membranes results in the specific transport of protons by bacteriorhodopsin.

If the changes in pH were generated exclusively by the transmembrane current protons pumped by bacteriorhodopsin and if these protons were accumulated in a nonleaky compartment, the change in proton concentration would simply be given by the time integral of the photocurrent. Thus,

$$\Delta[H] = \frac{L}{F} \int_0^t I(t)_{\text{light}} \, dt, \tag{6}$$

where F is Faraday's constant and L is Avogadro's number. The voltage recorded by the electrode would be

$$\Delta V = \frac{RT}{F} \ln \frac{[H]_i + \alpha \Delta[H]}{H_i}, \tag{7}$$

where $[H]_i$ is the initial or background concentration of protons and α represents the proton buffering ability of the medium:

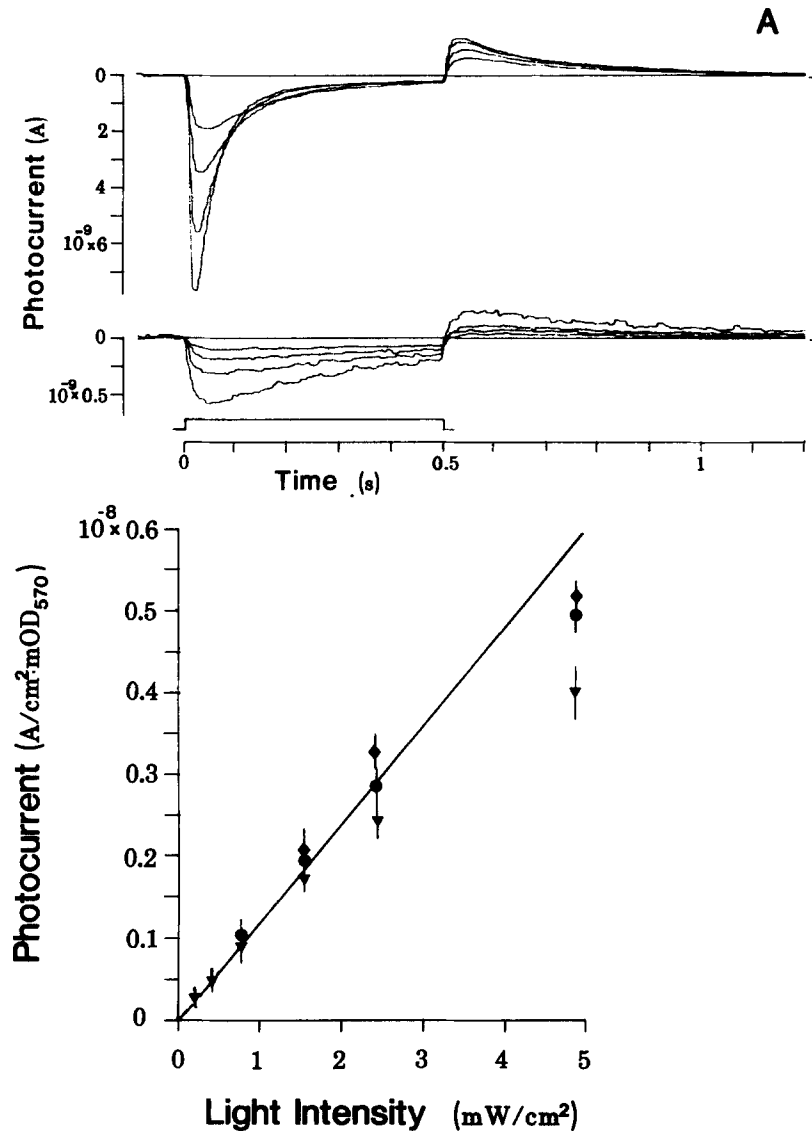$$\alpha = \frac{[H]^{\text{free}}}{[H]^{\text{total}}}. \tag{8}$$

FIGURE 11. A shows photocurrents measured in a 0.7 cm^2 membrane assembled from 7:1 bacteriorhodopsin:lipid films. The photocurrents were recorded in response to step illumination of 49, 30.9, 15.5, 7.75, 2.45, 1.55, 0.75, and 0.37 mW/cm^2. B shows photocurrents measured in a 2.3 × 10^{-2} cm^2 membrane assembled from 3.5:1 bacteriorhodopsin:lipid films in response to step illumination of 49, 30.9, 15.5, 7.75, 2.45 and 1.55 mW/cm^2. The graphs illustrate the dependence of the peak photocurrent on light intensity. Peak photocurrents are normalized by the area of the assembled membrane and its bacteriorhodopsin content. Data were collected from membranes of 2.3 × 10^{-2} cm^2 area assembled from either 7:1 (●) or 3.5:1 (◆) bacteriorhodopsin:lipid films, or from 0.7 cm^2 area assembled from 7:1 films (▼). Data points are the average of three to five membranes; error bars indicate ± SD.

However, this simple model is physically unreasonable in that the compartment into which protons are transported cannot be expected to be nonleaky. To analyze the photo-pH data, therefore, we simulated the pH responses with an analogue computer. We simply integrated experimentally recorded pho-
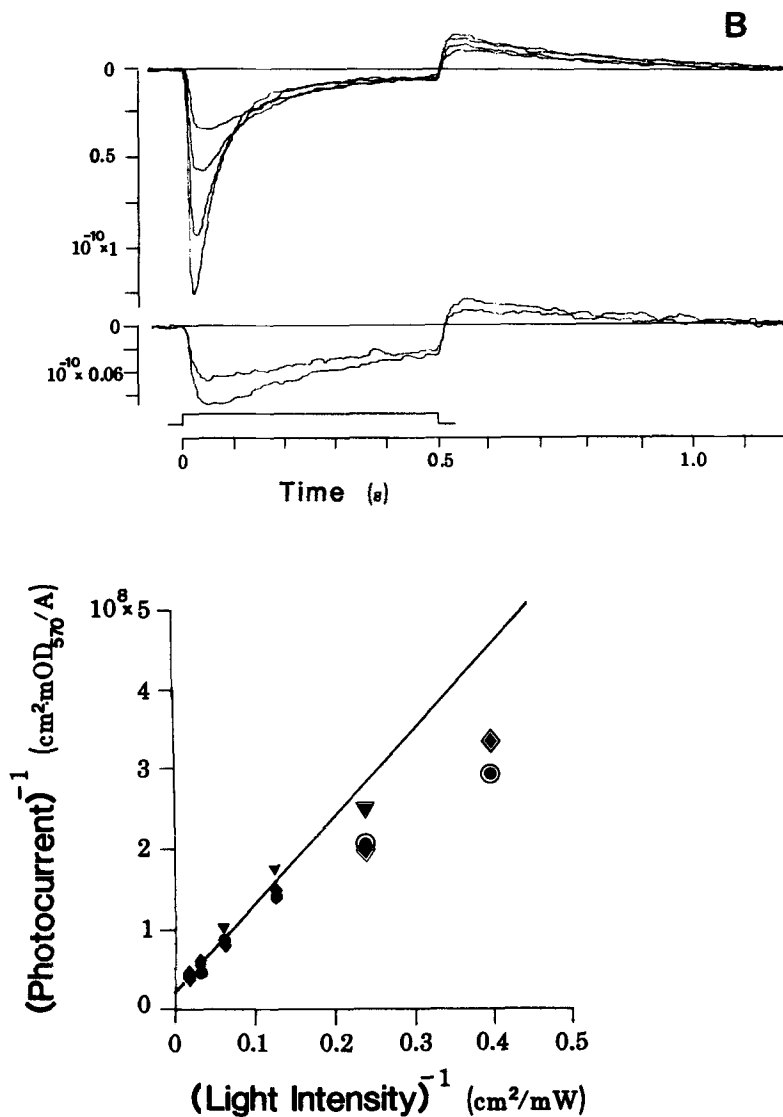

FIGURE 11.

tocurrents of various intensities through a leaky integrator and adjusted the "leak" to best match the recorded pH photoresponse. Fig. 12 illustrates both the perfect integral and the leaky integration of a set of photocurrents. The simulated photo-pH data shown in Fig. 12 match the experimental data

shown in Fig. 11. The adjusted leak rate necessary to match simulated and experimental data had a value which ranged, for all membranes tested, between 1 and 8% of the value of the light-activated rate of transport. This value was determined by quantitatively comparing the rate of rise at the onset of light of the experimental and simulated photo-pH data. With the integration data we were able to calculate the extent of the proton concentration
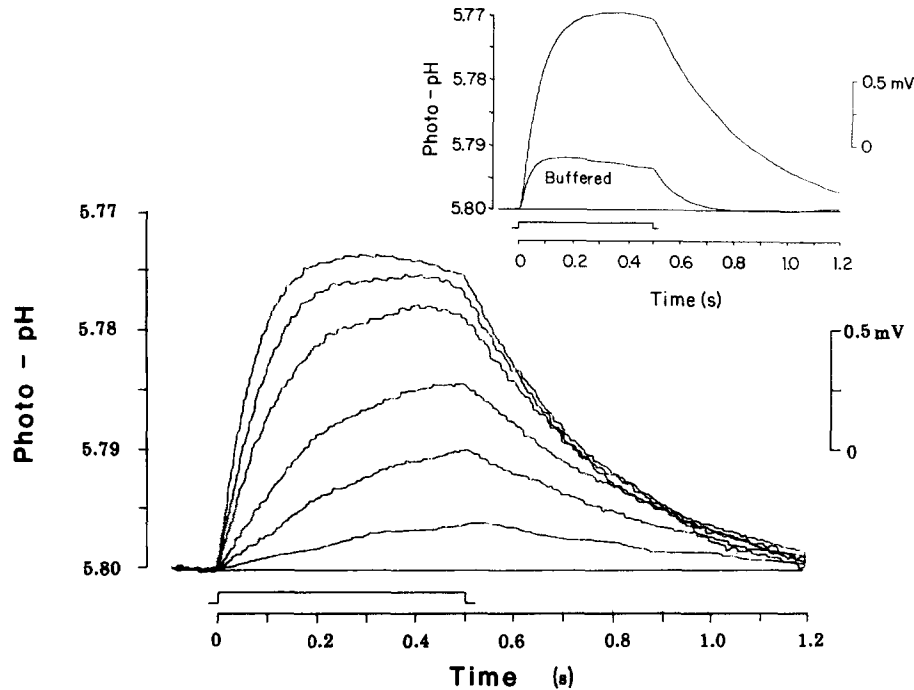

FIGURE 12. Light-induced changes in pH. Shown are the responses of a membrane assembled from 7:1 bacteriorhodopsin:lipid films in 4×10^{-4} M NaHCO$_3$, 4×10^{-4} M CdCl$_2$, pH 5.8. Stimulus intensities were 49, 30.9, 15.5, 7.75, 1.55, and 0.39 mW/cm^2. The inset demonstrates the effect of proton buffer solution on the light-induced change in pH in a different membrane. The photoresponse to a 49 mW/cm^2 intensity step of light was first recorded in 4×10^{-4} M NaHCO$_3$, 4×10^{-4} M CdCl$_2$, pH 5.8, 0.3 ml of 1 M cacodylic buffer, pH 5.8, was then added to the well in the Langmuir trough. The aqueous phase could not be stirred. After 15 minute's wait, the record labeled buffered was obtained in response to the same stimulus.

change expected to be produced by the photocurrent. In Table II, we compare this prediction (expressed in millivolts through the use of Eq. 7 with $\alpha = 0.04$, the value calculated for NaHCO$_3$ buffer [pK 6.1] at a 4×10^{-4} M concentration at pH 5.8) with the actual signal measured by the pH electrode. The substantial agreement of predicted and recorded data indicates that the pH photoresponse recorded is accounted for by the net transmembrane proton translocation by bacteriorhodopsin.

Stoichiometry of Proton Transport

The stoichiometry of the proton transport can be determined inasmuch as the amount and orientation of bacteriorhodopsin in the model system is known and since the photocurrent is all accounted for by the specific movement of protons. Fig. 13 illustrates the dependence of the peak photocurrent on light intensity for responses generated with 570-nm light stimuli. The data shown were recorded in membranes of different area assembled from 7:1 bacteriorhodopsin:lipid films. The absorbance of these films at 570 nm is 4×10^{-4} OD

TABLE II

COMPARISON OF PREDICTED AND OBSERVED PHOTO-pH
CHANGE

Light intensity,* ND filter	Observed pH electrode response‡	Predicted pH electrode response‖	Predicted change in [H]§
	μV	μV	mol/l
0	1,331±143	1,338±102	$84.5 \pm 6 \times 10^{-9}$
0.2	1,253±150	1,321±185	$83.4 \pm 11 \times 10^{-9}$
0.5	1,037±105	1,055±160	$66.3 \pm 10 \times 10;^{-9}$
0.8	737±176	779±150	$48.7 \pm 9 \times 10^{-9}$
1.0	708±80	627±105	$39.14 \pm 7 \times 10^{-9}$
1.3	541±50	416±97	$25.79 \pm 6 \times 10^{-9}$

* Given in units of logarithmic attenuation. Unattenuated light consisted of wavelengths longer than 470 nm and had intensity of 49 mW/cm^2.

‡ The amplitude of the response at $t = 185$ ms (peak amplitude). Data given are the average ± SEM of measurements in three different assembled membranes formed from 7:1 bacteriorhodopsin: soya PC interface films.

‖ The data used to predict the pH change were the average ± SEM obtained from the integral between 0 and 185 ms of photocurrents recorded in four separate assembled membranes formed from 7:1 bacteriorhodopsin: soya PC interface films.

§ The critical numbers used in these calculations are the volume in which the proton concentration change occurs and the buffering power of the solution in that volume. The critical volume we took to be the volume between the assembled membrane and the pH electrode surface. This volume is determined by the surface area of the electrode (12.7 cm^2) and the thickness of the nitrocellulose film (360 Å). The buffering power α of a 4×10^{-4} M solution of NaHCO$_3$ buffer (pK $= 6.1$) at pH $= 5.8$ is calculated to be 0.04.

(Hwang et al., 1977 *a*). In the linear range, the data from both membranes exhibit the same slope of $7.2 \pm 1 \times 10^{-24}$ A/photon delivered/s. Considering the absorbance of the membrane, this corresponds to $7.8 \pm 1 \times 10^{-21}$ A/photon absorbed/s. In Appendix II it is shown that in these membranes (where steady-state current is negligibly small), the measured peak photocurrent (I_0) is related to the pump photocurrent (I_{BRh}) by

$$I_{BRh} = I_0 \left(1 + \frac{C_1}{C_2}\right), \tag{9}$$

where C_2 (Table I) $= 0.15 \ \mu F/cm^2$. We will assume for the calculation that C_1, the capacitance of the purple membrane, is 1 $\mu F/cm^2$. This assumption is

arbitrary because no direct measurement is available. However, because purple membrane consists of a lipid bilayer of thickness comparable to that of other biological membranes, the choice of capacitance value is not unreasonable. The stoichiometry of the bacteriorhodopsin membrane is then $63 \pm 8 \times 10^{-21}$ A/photon absorbed/s or 0.39 ± 0.04 H^+/photon absorbed. In addition, $\sim 85 \pm 10\%$ of the molecules are oriented in the same direction (Hwang et al., 1977 a). If we include this correction, the stoichiometry of transport becomes 0.65 ± 0.06 H^+/photon absorbed.
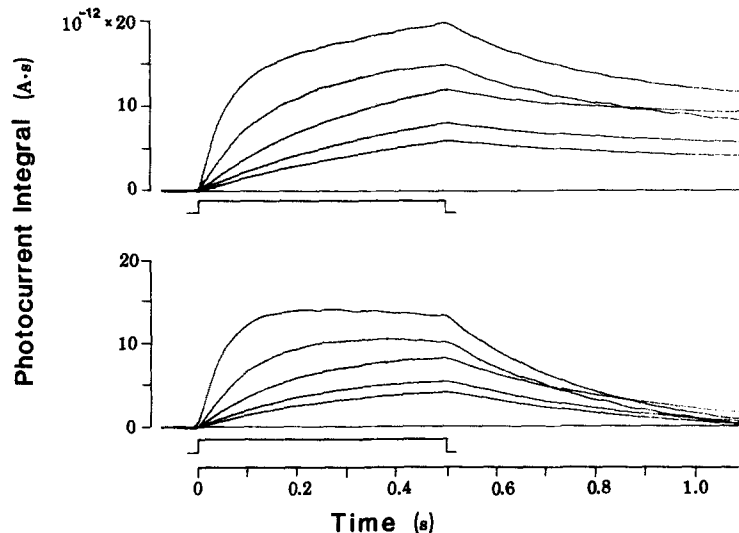

FIGURE 13. Analogue computer integration of photocurrents recorded in a membrane assembled from 7:1 bacteriorhodopsin:lipid film in 4×10^{-4} M $NaHCO_3$, 4×10^{-4} M $CdCl_2$, pH 5.8. The *top panel* shows the time integral of photocurrents recorded in response to steps of 49, 15.5, 4.9, 1.55, and 0.39 mW/cm^2 intensity. The *bottom panel* shows the integration of the same photocurrents through a leaky integrator. The value of the leak was selected to obtain waveforms that matched those experimentally recorded with the pH electrode. In this particular experiment the leak rate was $\sim 2\%$ of the light-induced rate of transport.

Light-induced Charge Displacement in Bacteriorhodopsin

Illumination of the assembled bacteriorhodopsin membranes by an intense, brief (10-μs) flash produces a transient photovoltage. A typical signal is shown in Fig. 14. This transient photovoltage exhibits no detectable latency, reaches a peak in about 80 μs, and proceeds to photovoltage that results from the net translocation of protons from one side of the membrane to the other, which can also be detected, as shown in Fig. 16. The transient photovoltage is of a polarity opposite to that which results from the net proton photocurrent. This transient voltage most probably arises from molecular charge displacements that occur upon photoexcitation of bacteriorhodopsin. Such light-induced

molecular charge displacements in purple membrane fragments, first described by Trissl and Montal (1977), have also been reported by Drachev et al. (1978) and Keszthelyi and Ormos (1980) in other experimental systems containing purple membrane fragments. In one such system, consisting of a dry multilayer film formed from purple membrane interface films, we have shown that charge displacement can be recorded upon photoexcitation not only of bacteriorhodopsin (BR_{510}), but also of M_{412}, N_{520} and O_{690} (Hwang et al., 1978). The observations made in the assembled membranes confirm that the charge displacements we have previously observed in dry systems occur in an aqueous medium and provide a possible experimental system for the determination of the physical mechanisms underlying these transient photovoltages.
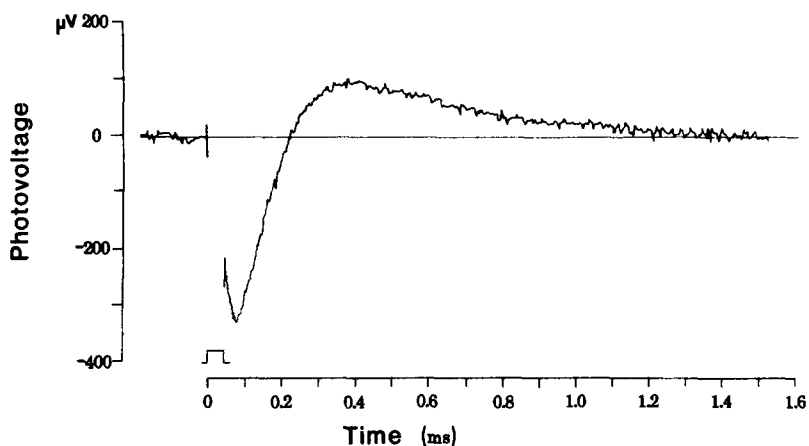

FIGURE 14.   Transient photovoltage recorded in response to a flash of ~ 10 μs duration in a 2.3×10^{-2} cm^2, 7:1 bacteriorhodopsin:lipid membrane. The record was interrupted during the duration of the stimulus flash to avoid recording the large electronic trigger artifact that occurs. The negative-going trace reveals a signal of no apparent latency preceding the polarization due to proton transport (positive signal).

DISCUSSION

We have described the assembly of planar films containing known amounts of oriented bacteriorhodopsin through the sequential transfer of two air-water interface films. The assembled membrane is supported on a hydrophilic and electrically conductive thin film of nitrocellulose. The formation of planar membranes through the assembly of interface films is not a novel concept. Takagi et al. (1965) pioneered the incorporation of biological proteins into lipid films by the simultaneous hydrophobic apposition of air-water interface films containing membrane fragments. Montal and Mueller (1972) improved on this concept and developed a method to form lipid bilayers from lipid monolayers and Montal (1974 and 1976) has further developed such techniques for the incorporation of membrane proteins (see also Schein et al. [1976] and Schindler and Rosenbusch [1978]). The assembly of films by the

sequential transfer of air-water interface films, first described by Blodgett (1935), has been extensively used as a tool in many areas of research. Hui et al. (1975) described the sequential assembly of two phospholipid monolayers onto a copper grid to form a bilayer whose structure was shown to be the same as that of biological membranes. We chose to develop the latter type of procedure, partly because of our failure with other methods, but also because we expected to attain better control of the assembled membrane through the sequential transfer of well-defined interface films.

The interface films used as building blocks in the formation of planar membranes must be well characterized in structure and function. Success with films in which proteins are structurally denatured or extensively aggregated would be improbable. In the experiments described here the bacteriorhodop-sin-containing interface films consist of oriented fragments of purple membrane separated by lipid monolayer (Hwang et al., 1977 a). If such films are to be used in a quantitative way, it is important to develop conditions in which membrane overlap on the surface is minimized.

The use of nitrocellulose supports for planar membranes, again, is not new. Possibly the first system ever designed to model transport in biological membranes is that of Abramson and Gray (1927), who impregnated films of collodion (an ether-ethanol solution of unpurified nitrocellulose) with crude phospholipids and studied the transport of water across them. While the work reported here was in progress, Tredgold and Elgamal (1979) described the formation of cytochrome oxidase–containing membranes through the sequential assembly of air-water interface films utilizing a technique similar in concept to that described here but carried out in a different manner. We selected nitrocellulose as the support for membrane assembly because (a) Neumann (1975) had shown that stearic acid monolayers exhibit the same transfer ratio and withdrawal contact angle when transferred onto nitrocellulose as when transferred onto glass or mica; and (b) the elegant work of Gregor and Sollner (1946), Neihof (1954), Lackshminarayanaiah and Shanes (1965), and Carnell and Cassidy (1961) had shown that through controlled experimental manipulation nitrocellulose films can be produced that exhibit well-defined and reproducible physical characteristics relative to their thickness, ion and water permeability, and ion selectivity. When nitrocellulose supports are used, therefore, it is important to define their physical character- istics, since these affect the electrical signal recorded across the assembled membranes. The thickness of the polymeric film, for example, can be con- trolled in part by the concentration of nitrocellulose and the solvent used in casting (Carnell and Cassidy, 1961; Lackshminarayanaiah and Shanes 1965). The condition we selected, 1% in isoamyacetate, produced films that are thin yet sufficiently strong to support the pressure to which they are subjected throughout the assembly routine. The electrical resistance of the support can be controlled to a limited extent by the technique of film casting. The Carnell- Cassidy method produces films of higher resistance (less porosity) than the Lackshminarayanaiah-Shanes method (Table I, and Lackshminarayanaiah [1965]). This latter technique is preferred, therefore, when the solution bathing

the assembled membrane from the support film side is to be repeatedly changed in an experiment and when the access resistance to the membrane must be low.

The membranes assembled from purple membrane films and lipid interface films are extremely stable if care is taken to avoid mechanical vibrations. Data were routinely collected for 4–6 h. The protein stability arises from the fact that, in contrast with studies of other membrane proteins, we have not "disassembled and reconstituted" a membrane, but simply assembled membrane fragments into a new orderly structure. The same approach is being used for the assembly of membranes containing other proteins by first forming adequate interface films. These interface films can be formed, for example, by the osmotic lysis of vesicles of both native and reconstituted membranes on the aqueous surface (Korenbrot and Pramik [1977] and Korenbrot and Jones [1979]; see also Schindler and Rosenbusch [1978] and Verger and Pattus [1976]).

The resistance of the bacteriorhodopsin assembled membranes is relatively low ($\sim 10^5$ Ω cm^2) when compared with lipid bilayers ($\sim 10^8$–10^9 Ω cm^2). This lower resistance may represent the resistance of the purple membrane itself, but we think that it more likely represents a leak between the edge of the purple membrane fragments and the assembled lipid bilayer. Purple membrane fragments are rigid, crystalline structures that are now surrounded by a fluid, pure lipid assembly. The edges of rigid and fluid domains in lipid bilayers have been shown to be leaky to ions (Papahadjopoulos et al., 1973; Marsh et al., 1976), and similar leaks should exist between the lipid and purple membrane domains. Indeed, membranes assembled from pure phospholipid monolayers exhibit higher resistance ($\sim 10^7$ Ω cm^2) than those containing purple membrane fragments.

The assembled bacteriorhodopsin membranes permit the measurement in the same system of light-induced changes in current, voltage, and pH. Action spectra demonstrate that these changes result from the photoexcitation of the light-adapted state of bacteriorhodopsin. The photocurrent amplitude increases linearly with light intensity at low light intensities (<3.5 mW/cm^2) and approaches a saturating value at high light intensities. This is in agreement with the observations of Herrmann and Rayfield (1978) and Bamberg et al. (1979). The stoichiometry of proton transport we have calculated is 0.65 $\pm$ 0.09 H$^+$/absorbed photon, based on an assumed membrane capacitance. In intact cells, estimates of the stoichiometry of the proton pump have been given to be between 0.4 and 0.7 H$^+$/photon absorbed (Bogomolni, 1977; Stoeckenius et al., 1979). The quantum yield of bacteriorhodopsin excitation has been measured to be about 0.3 (Becher and Ebrey, 1977). Taking this quantum yield, our calculated stoichiometry of transport indicates that about 2 protons/ excited bacteriorhodopsin molecule are transported in the assembled planar membranes. Govindjee et al. (1980) have reported that in isolated purple membrane fragments the number of protons transported for every excited bacteriorhodopsin molecule can vary between ~ 0.64 and ~ 1.8, depending on the salt concentration. In contrast, they found that purple membrane frag-

ments incorporated in vesicle lipid membranes (proteoliposomes) transport two protons for every excited bacteriorhodopsin molecule at all salt concentrations. In the assembled membranes described here, the stoichiometry of proton transport by bacteriorhodopsin is also independent of salt concentration. This is best demonstrated by the fact that the capacitative peak of the observed photocurrent, a direct measure of pump current (Eq. 9), does not change when the salt concentration in the solutions bathing the membrane is changed (see Fig. 6).

One particular advantage of the membrane assembly described here is the control of membrane area, which permits the study of large membranes. With purple membrane, the increase in membrane area reveals the functional independence of the bacteriorhodopsin molecules. Increasing membrane area (or varying protein concentration for a given area) results in photocurrents that are linearly scaled in amplitude with area (or concentration). That is, increasing the number of pumping elements, i.e., bacteriorhodopsin molecules, results in a simple linear recruitment of independent elements, with no evidence of cooperativity.

The assembled membranes are accessible to the aqueous phase on both of its surfaces, since the polymeric support facing one such surface is sufficiently porous to allow the rapid and complete exchange of solutions. Moreover, the access resistance of the support can be controlled. Nonetheless, clearly one of the limitations of the assembly procedure is that the solid support is not simply an aqueous phase. Thus, any quantitative analysis of data recorded in membranes assembled on a support must consider the electrical features of the support itself. A special advantage of the assembly system in the study of photochemical systems such as bacteriorhodopsin is that the large size and stability of the membranes will make it possible to experimentally correlate the transport mechanism of the protein with photoinduced spectroscopic changes, for example, in understanding the mechanisms of the transient photovoltages described here. A truly simple and universal method for incorporating biological membrane-bound proteins into planar films is not yet at hand. On the other hand, the method described here offers some advantages, and we hope it opens a different avenue into these problems.

APPENDIX I

Gaines (1961 and 1966) has shown that hexadecane evaporates from mixed stearic acid–hexadecane films formed at an air-water interface. The evaporation occurs at a rate that can reasonably be estimated from the rate of evaporation in air from the surface of pure hydrocarbon. Of course, as Robbins and LaMer (1960) have argued, some of the solvent must also disappear by diffusion into the subphase. Gaines (1961) has indicated that the rate of loss of hexadecane from a surface film can be determined by measuring at a constant surface pressure the area of the film as a function of time. Fig. 15 presents surface-pressure isotherms of interface films formed from soya PC and hexadecane at various mole ratios. Also shown are a measurement of the film area at 30 mN/m as a function of time. The data shown are entirely analogous to those obtained by Gaines (1961) for fatty acid–hexadecane films. Two successive processes can be distinguished in the kinetic curves of Fig. 15. First, the area remains constant for a period of time that depends on the amount of hydrocarbon initially

present. During this time excess hydrocarbon evaporates until a true "mixed" film is left. At this point in time, further solvent disappearance results in a loss of film area. Gaines reported, and we confirm here, that the rate of area loss follows a first-order rate process:

$$A(t) = [A(t_0) - A(t_\infty)] e^{-k(t - t_0)},$$

where $A(t_0)$ and $A(t_\infty)$ are the surface areas at time t_0 and at the end of the experiment, respectively, k is a rate constant, and t_0 is the duration of the first process of excess solvent evaporation. As expected, t_0 is a function of the initial hexadecane:soya PC mole ratio, but the rate constant k is not (Table III). For the assembly experiments reported here, we chose a hexadecane:soya PC mole ratio of 32:1, for which t_0 is 10–14 min.
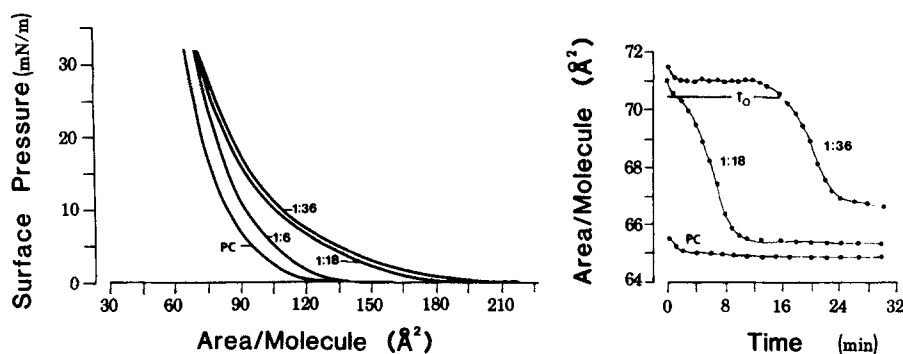

FIGURE 15. The surface pressure–area diagram on the left shows isotherms recorded at room temperature over a 4×10^{-4} M $NaHCO_3$, 4×10^{-4} M $CdCl_2$ subphase for interface films spread from hexane and consisting of soya PC or mixtures of soya PC:hexadecane in the mole ratio indicated in the figure. After a surface pressure of 30 mN/m was reached, the servoloop feature of the surface balance was engaged, and the change in area as a function of time was measured for each of the films. Typical data are shown in the diagram on the right. The rapid initial loss of area observed in all films is most probably due to the evaporation of hexane. The films containing hexadecane, after an initial time period t_0, show an exponential loss of area and approach a final value similar to that of the pure phospholipid film. The accuracy of the measurement is ± 1 $\text{Å}^2/$ molecule

APPENDIX II

The analysis of the circuit shown in Fig. 5 under conditions of short-circuit current measurements has been carried out in detail by Herrmann and Rayfield (1978) and Bamberg et al. (1979), whose papers should be consulted for full details. Here we follow them.

I_{BRh} denotes the current generated by light activation of bacteriorhodopsin. The actual current across the purple membrane, I_m, was found by Herrmann and Rayfield (1978) and Bamberg et al. (1979) to be proportional to the voltage across the membrane, V_m, thus,

$$I_m = I_{BRh} \left(1 - \frac{V_m}{V_c}\right), \tag{A1}$$

where V_c is a constant. It must be noted that in this formulation, I_{BRh} depends on light intensity but not on V_m.

From the equivalent circuit, it follows that

$$I_m(V_m,t) = \frac{V_m}{R} + C\frac{dV_m}{dt},$$ (A2)

where

$$\frac{1}{R} = \frac{1}{R_1} + \frac{1}{R_2} \quad\text{and}\quad C = C_1 + C_2.$$ (A3)

substituting Eq. A1 in Eq. A2 yields

$$I_{BRh}(t) = V_m\left(\frac{1}{R} + \frac{I_{BRh}}{V_c}\right) + C\frac{dV_m}{dt}.$$ (A4)

Upon illumination, $I_{BRh}(t)$ takes a constant value I_{BRh} for the duration, t_0, of the light pulse. The value of I_{BRh}, of course, is proportional to light intensity. Integration of Eq. A4 under these conditions yields

$$V_m(t) = I_{BRh}R'(1 - e^{-t/\tau'}),$$ (A5)

TABLE III

RATE OF HEXADECANE DISAPPEARANCE FROM MIXED
MONOLAYERS

Monolayer composition of soya PC:hexadecane	t_0	k
mole ratio	*min*	*min*$^{-1}$
1:6	1	1.68
1:18	5.5	1.52
1:36	16	1.69

where

$$\frac{1}{R'} = \frac{1}{R} + \frac{I_0}{V_c} \quad\text{and}\quad \tau' = R'C,$$ (A6)

Since the observed current, I_0, is given by

$$I_0 = i_2 = \frac{V_m}{R_2} + C_2\frac{dV_m}{dt},$$ (A7)

it follows that

$$I_0 = I_{BRh}\frac{C_2}{C}(A + (1 - A)e^{-t/\tau'}),$$ (A8)

where $A = \dfrac{\tau'}{\tau_2}$ and $\tau_2 = R_2C_2$.

Eq. A8 describes the kinetics of the photocurrent for the duration of the light pulse. At the termination of the light pulse, the observed photocurrent should be described by:

$$I_0 = \frac{V_m}{R_2}(1 - \tau_2/\tau)e^{-t/\tau},$$ (A9)

where $\tau = RC$. Eqs. A8 and A9 described well the experimentally observed photocurrents as described in the text.

The decay time constant of the observed photocurrent can now be more fully analyzed. It is apparent from the recorded wave forms (see Figs. 3 and 11) that the decay constant of the photocurrent, τ', is proportional to light intensity. Such behavior is indeed expected, as Eq. A6 demonstrates. The dependency of $1/\tau'$ on light intensity should be the same as that exhibited by I_0. Moreover, the light dependency of $1/\tau'$ should be independent of the area or bacteriorhodopsin content of the assembled membranes. This is indeed the case. Fig. 16 shows that $1/\tau'$ varies linearly with light intensity at low light intensities (<3.5 mW/cm^2) and with a rectangular-hyperbola like dependence at higher light levels. This is the same dependency on light exhibited by I_0 (see Figs. 8 and 11).
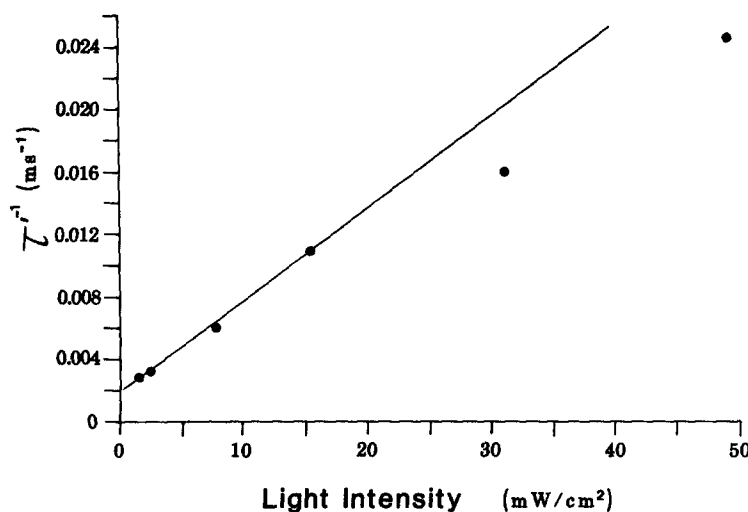

FIGURE 16. Relation between the decay time constant of the photocurrent measured in 4×10^{-4} M NaHCO$_3$, 4×10^{-4} M CdCl$_2$, pH 5.8, and light intensity. The data were obtained in a 2.3×10^{-2} cm^2 7:1 bacteriorhodopsin: lipid membrane. The functional dependence on light intensity of the time constant is the same as that shown by the peak photocurrent amplitude.

REFERENCES

Abramson, H. A., and S. H. Gray. 1927. The diffusion of water into lecithin-collodion membranes. *J. Biol. Chem.* **73:**459-462.

Bakker, E. P., H. Rottenberg, and R. Caplan. 1976. An estimation of the light induced electrochemical potential difference of protons across the membrane of *Halobacterium halobium.* *Biochim. Biophys. Acta.* **440:**557-572.

BAMBERG, E., H.-J. APELL, N. DENCHER, W. SPERLING, H. STIEVE, and P. LAUGER. 1979. Photocurrent generated by bacteriorhodopsin on planar bilayer membranes. *Biophys. Struct. Mech.* 5:277–292.

BECHER, B., and T. G. EBREY. 1977. The quantum efficiency for the photochemical conversion of the purple membrane protein. *Biophys. J.* 17:185–191.

BLODGETT, K. B. 1935. Films built by depositing successive monomolecular layers on a solid surface. *J. Am. Chem. Soc.* 57:1007–1022.

BLOK, M. C., K. I. HELLINGWERF, and K. VAN DAM. 1977. Reconstitution of bacteriorhodopsin in a Millipore filter system. *FEBS (Fed. Eur. Biochem. Soc.) Lett.* 76:45–50.

BLOK, M. C., and K. VAN DAM. 1978. Association of bacteriorhodopsin containing phospholipid vesicles with phospholipid-impregnated Millipore filters. *Biochim. Biophys. Acta.* 507:48–61.

BOGOMOLNI, R. 1977. Light energy conservation processes in *Halobacterium halobium* cells. *Fed. Proc.* 36:1833–1839.

CARNELL, P. H. 1965. Preparation of thin polymer films *J. Appl. Polymer Sci.* 9:1863–1872.

CARNELL, P. H., and H. G. CASSIDY. 1961. The properties of membranes. *J. Polymer Sci.* 55:233–249.

DANCSHAZY, Z., and B. KARVALY. 1976. Incorporation of bacteriorhodopsin into a bilayer lipid membrane: a photoelectric-spectroscopic study. *FEBS (Fed. Eur. Biochem. Soc.) Lett.* 72:136–138.

DRACHEV, L. A., V. N. FROLOV, A. D. KAULEN, E. A. LIBERMAN, S. A. OSTRUMOV, U. G. PLAKUNOVA, A. Y. SEMENOU, and V. P. SKULACHEV. 1976. Reconstitution of biological molecular generators of electric current. *J. Biol. Chem.* 251:7059–7065.

DRACHEV, L. A., A. D. KAULEN, S. A. OSTRUMOV, and V. P. SKULACHEV. 1974. Electrogenesis by bacteriorhodopsin incorporated in a planar phospholipid membrane. *FEBS (Fed. Eur. Biochem. Soc.) Lett.* 39:43–45.

DRACHEV, L. A., A. D. KAULEN, and V. P. SKULACHEV. 1978. Time resolution of the intermediate steps in the bacteriorhodopsin-linked electrogenesis. *FEBS (Fed. Eur. Biochem. Soc.) Lett.* 87:161–167.

GAINES, G. L. 1961. On the retention of solvent in monolayers of fatty acids spread on water surfaces. *J. Phys. Chem.* 65:382–383.

GAINES, G. L. 1966. Insoluble monolayers at liquid-gas interfaces. Interscience, New York.

GOVINDJEE, R., T. G. EBREY, and A. R. CROFTS. 1980. The quantum efficiency of proton pumping by the purple membrane of *Halobacterium halobium. Biophys. J.* 30:231–234.

GREGOR, H. P., and K. SOLLNER. 1946. Improved methods of preparation of "permselectivity" collodion membranes combining extreme ionic selectivity with high permeability. *J. Phys. Chem.* 50:53–70.

HENDERSON, R. 1977. The purple membrane from *Halobacterium halobium. Annu. Rev. Biophys. Bioeng.* 6:87–109.

HERRMANN, T. R., and G. W. RAYFIELD, 1978. The electrical response to light of bacteriorhodopsin in planar membranes. *Biophys. J.* 21:111–125.

HUI, S. W., M. COWDEN, D. PAPAHADJOPOULOS, and D. F. PARSONS. 1975. Electron diffraction study of hydrated single bilayers: effects of temperatures, hydration and surface pressure of the 'precursor' monolayer. *Biochim. Biophys. Acta.* 382:265–275.

HWANG, S. B., J. I. KORENBROT, and W. STOECKENIUS. 1977 a. Structural and spectroscopic characteristics of bacteriorhodopsin in air-water interface films. *J. Membr. Biol.* 36:115–135.

HWANG, S. B., J. I. KORENBROT, and W. STOECKENIUS. 1977 b. Proton transport by bacteriorhodopsin through an interface film. *J. Membr. Biol.* 36:137–158.

HWANG, S. B., J. I. KORENBROT, and W. STOECKENIUS. 1978. Transient photovoltages in purple

membrane multilayers: charge displacement in bacteriorhodopsin and its photointermediates. *Biochim. Biophys. Acta.* **509:**300–317.

KESZTHELYI, L., and P. ORMOS. 1980. Electrical signals associated with the photocycle of bacteriorhodopsin. *FEBS (Fed. Eur. Biochem. Soc.) Lett.* **109:**189–193.

KORENBROT, J. I. 1977. Ion transport in membranes: incorporation of biological ion translocating proteins in model membrane systems. *Annu. Rev. Physiol.* **39:**19–49.

KORENBROT, J. I., and O. JONES. 1979. Linear dichroism of rhodopsin in air-water interface films. *J. Membr. Biol.* **46:**239–254.

KORENBROT, J. I., and M. J. PRAMIK. 1977. Formation, structure, and spectrophotometry of air-water interface films containing rhodopsin. *J. Membr. Biol.* **37:**235–262.

LACKSHMINARAYANAIAH, N. 1965. Preparation and characterization of thin parlodion membranes. *J. Appl. Polymer Sci.* **9:**1285–1290.

LACKSHMINARAYANAIAH, N., and A. M. SHANES. 1965. Electrochemical properties of thin parlodion membranes. *J. Appl. Polymer Sci.* **9:**689–706.

MARSH, D., A. WATTS, and P. F. KNOWLES. 1976. Evidence of phase boundary lipid. Permeability of tempo-choline into dimyristoilphosphatidyl choline vesicles at the phase transition. *Biochemistry.* **15:**3570–3578.

MONTAL, M. 1974. Lipid-protein assembly and the reconstitution of biological membranes. *In*: Perspectives in Membrane Biology. S. O. Estrada and C. Gitler, Editors, Academic Press, Inc., New York. 591–622.

MONTAL, M. 1976. Experimental membranes and mechanisms of bioenergy-transduction. *Annu. Rev. Biophys. Bioeng.* **5:**119–135.

MONTAL, M., and P. MUELLER. 1972. Formation of bimolecular membranes from lipid monolayers and a study of their electrical properties. *Proc. Natl. Acad. Sci. U. S. A.* **69:**3561–3566.

NEIHOF, R. 1954. The preparation and properties of strong acid type collodion-base membranes. *J. Phys. Chem.* **58:**916–925.

NEUMAN, R. D. 1975. Langmuir-Blodgett monolayer deposition on collodion. *J. Colloid Interface Sci.* **50:**602–605.

OESTERHELT, D. 1975. The purple membrane of *Halobacterium halobium*: a new system for light energy conversion. *Ciba Found. Symp.* **31** (new series):147–161.

OESTERHELT, D., and W. STOECKENIUS. 1971. Rhodopsin-like protein from the pruple membrane of *Halobacterium halobium. Nat. New Biol.* **233:**149–152.

OESTERHELT, D., and W. STOECKENIUS. 1973. Function of a new photoreceptor membrane. *Proc. Natl. Acad. Sci. U. S. A.* **70:**2853–2857.

OESTERHELT, D., and W. STOECKENIUS. 1974. Isolation of the cell membrane of *Halobacterium halobium* and its fraction into red and purple membrane. *Methods Enzymol.* **31:**667–678.

PAPAHADJOPOULOS, D., K. JACOBSON, S. NIR, and T. ISAC. 1973. Phase transitions in phospholipid vesicles. Fluorescence polarization and permeability measurements concerning the effect of temperature and cholesterol. *Biochim. Biophys. Acta.* **311:**330–348.

POCKRAND, I., J. D. SWALEN, J. G. GORDON, and M. R. PHILPOTT. 1977. Surface plasmon spectroscopy of organic monolayer asemblies. *Surface Sci.* **74:**237–244.

ROBBINS, M. L., and V. K. LAMER. 1960. The effect of the spreading solvent on the properties of monolayers. *J. Colloid Sci.* **15:**123–154.

ROBINSON, R. A., and R. H. STOKES. 1959. Electrolyte Solutions. Butterworth & Co., Ltd., London.

SCHEIN, S. J., M. COLOMBINI, and A. FINKELSTEIN. 1976. Reconstitution in planar lipid bilayers of a voltage dependent anion-selective channel obtained from *Paramecium* mitochondria. *J.*

Membr. Biol. **30:**99–120.

SCHINDLER, H. G., and J. P. ROSENBUSCH. 1978. Matrix protein from *Escherichia coli* outer membranes forms voltage-controlled channels in lipid bilayers. *Proc. Natl. Acad. Sci. U. S. A.* **75:**3751–3755.

SCHRECKENBACH, T. H. 1978. The properties of bacteriorhodopsin and its incorporation into artificial systems. *In* Photosynthesis in relation to model systems. J. Barber, editor. Elsevier/North Holland, Amsterdam.

SHIEH, P., and L. PACKER. 1976. Photo-induced potentials across a polymer stabilized planar membrane in the presence of bacteriorhodopsin. *Biochem. Biophys. Res. Commun.* **71:**603–609.

STOECKENIUS, W., R. H. LOZIER, and R. A. BOGOMOLNI. 1979. Bacteriorhodopsin and the purple membrane of *Halobacteria. Biochim. Biophys. Acta.* **505:**215–278.

TAKAGI, M., AZUMA, K., and V. KISHIMOTO. 1965. A new method for the formation of bilayer membranes in aqueous solution. *Annu. Rep. Biol. Works Fac. Sci. Osaka Univ.* **13:**107–110.

TREDGOLD, R. H., and M. ELGAMAL. 1979. A study of the incorporation of cytochrome oxidase into planar synthetic membranes. *Biochim. Biophys. Acta.* **555:**381–387.

TRISSL, H.-W., and M. MONTAL. 1977. Electric demonstration of rapid light-induced conformational changes in bacteriorhodopsin. *Nature (Lond.).* **266:**655–657.

VERGER, R., and F. PATTUS. 1976. Spreading of membranes at the air/water interface. *Chem. Phys. Lipids.* **16:**285–291.

WEAST, R. C. 1971. Handbook of Chemistry and Physics. Chemical Rubber Co.

WHITE, S. H. 1978. Studies on the physical chemistry of planar bilayer membranes using high-precision measurements of specific capacitance. *Ann. N. Y. Acad. Sci.* **303:**243–265.

WHITE, S. H., D. C. PETERSEN, S. SIMON, and M. YAFUSO. 1976. Formation of planar bilayer membranes from lipid monolayers. A critique. *Biophys. J.* **16:**481–489.